Proc. of the International Conference on Mechanochemistry and Mechanical Alloying, Kraków, Poland, June 22–26, 2014

Electrochemical and Corrosion Behavior of Nanocrystalline TiNi-Based Alloys and Composite

M. Balcerzak* and M. Jurczyk
Institute of Materials Science and Engineering, Poznań University of Technology,
pl. M. Skłodowskiej-Curie 5, 60-965 Poznań, Poland

In this work TiNi-based nanocrystalline alloys and composite were produced by mechanical alloying process with subsequent annealing at 750 °C for 0.5 h. Mechanical alloying was performed in a SPEX 8000 Mixer Mill. TiNi alloy was chemically modified by Ag elemental powder. Silver content equaled 5 wt%. X-ray diffraction analyses revealed formation of TiNi main phase after annealing. Additionally, two minor phases Ti_2Ni and $TiNi_3$ were detected for unmodified alloy. Crystallites of obtained powders were nanosized. Corrosion and electrochemical measurements were performed in 6 M KOH solution. All synthesized materials were used as negative electrode for Ni-MH_x batteries. Ag addition positively affects on stability of discharge capacity of TiNi alloy during of charge/discharge tests.

DOI: 10.12693/APhysPolA.126.888
PACS: 82.47.Cb, 88.30.rd

1. Introduction

Titanium-based hydrogen storage alloys have been considered as candidates for hydrogen storage and for negative electrodes in Ni-MH_x batteries. TiNi alloy absorb and desorb hydrogen at room temperature. This alloy revealed a discharge capacity equaled 150 mAh/g at a discharge current of 30 mAh/g. Application of microcrystalline TiNi material in metal–hydrogen systems is limited due to poor absorption/desorption kinetics and complicated activation procedure [1–3].

Chemical composition, microstructure of material and size of alloy crystals are one of the most important factors in metal–hydrogen systems. Ti-Ni type alloys can be produced by mechanical alloying (MA). This process which consist of repeated fracturing, mixing and cold welding provides formation of new nanostructured, non-equilibrium alloys [4]. Nanocrystalline TiNi alloy obtained by MA was studied by us in the past. Electrochemical discharge capacity was higher than for microcrystalline alloy and amounted 171 mAh/g. Improvement of mentioned properties is caused by reduction of powder size and creation of new clean surfaces [5].

Electrochemical properties of alloys for Ni-MH_x batteries can be also improved by chemical modification. Replacement of Ni element by transition metals may improve activation properties of TiNi alloy [1, 2, 4]. Addition of Pd and multiwalled carbon nanotubes positively influences electrochemical properties and improves cycle stability of electrode [6].

Silver can be also used to ameliorate discharge capacity of Ni-MH_x electrode. Shin et al. sintered $ZrMn_{0.6}V_{0.2}Co_{0.1}Ni_{1.2}$ with Ag to form pellet. Discharge capacity was also related to content of Ag in studied material [7]. Positive effect of silver addition was also observed in La-rich AB_5-type alloy. Ag affected on electrochemical reduction reaction rate of oxygen and cycle life of hydrogen storage [8].

In this work structure, agglomerate size and morphology, corrosion and electrochemical properties in 6 M KOH were measured. This paper is a continuation of our previous work. To the best of our knowledge, there are no reports on chemical modification of TiNi alloy by Ag element in order to improve electrochemical properties of electrode for Ni-MH_x batteries.

2. Experimental details

All materials were synthesized under an argon atmosphere by MA process performed in SPEX 8000 Mixer Mill. Every powder milling lasted 8 h. The purity of Ti, Ni, and Ag elemental powders used in MA was at least 99.9%. Detailed description of synthesis procedure was described in our previous works [5, 6]. In this we synthesized two materials: pure TiNi alloy and chemically modified TiNi alloy with 5 wt% of Ag added to elemental powder mixture before MA. Performed synthesis leads to formation of amorphous materials [5, 6]. Obtained powders were additionally annealed in argon atmosphere at 750 °C for 0.5 h to form TiNi CsCl-type structure. In order to verify another way of chemical modification TiNi-based composite was produced. This composite was done by 5 min mixing of MA and annealed TiNi alloy with 5 wt% of Ag in SPEX 8000 Mixer Mill.

To facilitate the reading of work obtained materials were labeled as follows:

- TiNi alloy without changes is labeled as TiNi,
- TiNi with 5 wt% of Ag nanocrystalline alloy is labeled as TiNi+Ag,
- Composite of TiNi alloy with 5 wt% of Ag elemental powder is labeled as TiNi+(Ag).

*corresponding author; e-mail: mateusz.balcerzak@put.poznan.pl

Structure, microstructure, and morphology of materials were studied by X-ray diffraction (XRD) using Cu K_α and scanning electron microscopy (SEM). Average crystallite size were calculated using the Scherrer equation. Based on SEM pictures particle size dimension distribution histograms were made. Each of histogram was made by counting about one thousand of crystal agglomerates.

Corrosion resistance behavior was examined during potentiodynamic tests in 6 M KOH solution with scanning range and speed –1.5 to 1 V and 1 mV/s, respectively, on Solatron 1285 potentiostat.

For electrochemical measurements obtained materials were mixed with 10 wt% additional NI powder and cold pressed under 800 MPa to form pellets. This pellets were used as negative electrodes in Ni-MH_x systems. Electrochemical measurements were performed in 6 M KOH solution using Multi-channel Battery Interface ATLAS 0461. Electrodes were charged and discharged at 40 MA/g. A cut-off potential vs. Hg/HgO/6 M KOH was –0.7 V. Cycle stability was evaluated by capacity retaining rate after 18th cycle

$$R_{\mathrm{h}} = \frac{C_{18}}{C_{\max}} \times 100\%, \tag{1}$$

where C_{18} and $C_{\max}$ are discharge capacities at the 18th cycle and maximum discharge capacity, respectively. Fully description of activation procedure and electrochemical measurements were described in our previous papers [5, 6].

3. Results and discussions

TiNi-based materials were characterized by XRD, SEM, corrosion and electrochemical measurements. 8 hours of mechanical alloying of Ti and Ni elemental powders lead to formation of amorphous phase without creation of any new crystalline phase [6]. Addition of Ag to mixture of elemental powders did not affect MA process (not shown here). Amorphous powders were annealed at 750 °C for 0.5 h. Figure 1 shows XRD spectra of obtained materials. The most intense peaks are related to presence of TiNi phase. Additionally to this main phase two minor phases were detected: Ti_2Ni and $TiNi_3$. On XRD pattern assigned to TiNi+Ag small peaks associated with presence of Ag crystals are visible. The same peaks were also visible on XRD spectra related to TiNi+(Ag) composite (Fig. 1c). However, the intensity of these peaks were much higher for TiNi based composite. Taking into account that both materials have the same amount of silver, we think that part of silver in TiNi+Ag alloy could react with Ti and Ni creating TiNi based phase (TiNi, Ti_2Ni, $TiNi_3$). Rest of elemental Ag did not react with other elements which is visible on XRD spectra. Based on XRD date, average crystalline size were calculated using the Scherrer equation. Silver addition does not significantly affect the crystallite size which equaled 26 and 28 nm for unmodified and modified alloys, respectively (Table I).

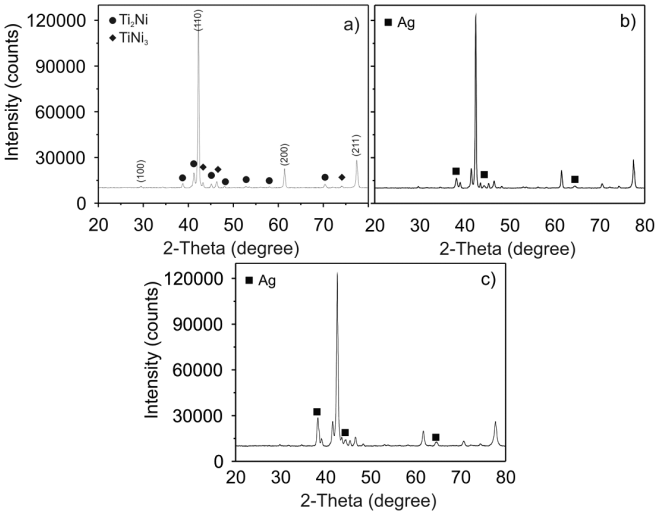

Fig. 1. XRD spectra of obtained powders of: (a) TiNi alloy, (b) TiNi+Ag, (c) TiNi+(Ag).

TABLE I

Crystallites size and average particle size of TiNi-based materials.

Composition	Crystallites size of annealed powders [nm]	Average agglomerates size of annealed powders [μm]
TiNi	26	25.5
TiNi+Ag	28	26.7

Figure 2 shows SEM pictures of TiNi and TiNi+Ag alloys. In both cases crystallite agglomerates had size from a few to one hundred of μm. MA and annealed materials had cleavage fracture morphology (Fig. 2a). Based on SEM pictures particle size dimension distribution histograms were made (Fig. 3). Most of agglomerates had size less than 50 μm. Average size of agglomerates is similar for TiNi and TiNi+Ag alloys and equaled a little bit more than 25 μm (Table I). Particle size dimension distribution of TiNi+Ag is more uniform.

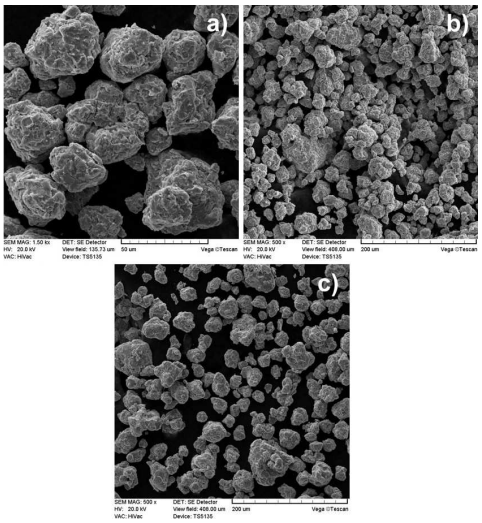

Fig. 2. SEM picture of TiNi (a,b) and TiNi+Ag (c).

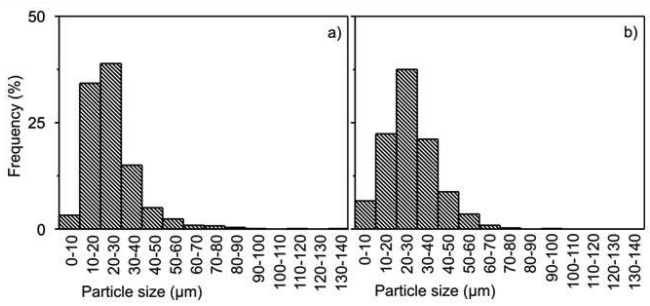

Fig. 3. Particle size dimension distribution histograms of: (a) TiNi, (b) TiNi+Ag.

The potentiodynamic polarization behavior of the uncharged studied alloys is given in Fig. 4. Curves had a very similar shape for all tested materials. Initially occurring area of resistance is followed by active dissolution of formed hydroxide layer. Then, the passivation process is observed during which the hydroxide layer is rapidly formed. The hydroxidation process has been disturbed for some reason, resulting in a creation of new clean surface. The surface was quickly hydroxidized to reach the passive state. Corrosion current for all of the powders is summarized in Table II. It is shown that Ag in TiNi alloy and composite improves the corrosion resistance of materials in alkaline solution. The best corrosion resistance was observed for TiNi+(Ag) composite. This slight improvement of corrosion properties probably resulted from suppressed pulverization of electrode due to the anticorrosion effect of silver addition.

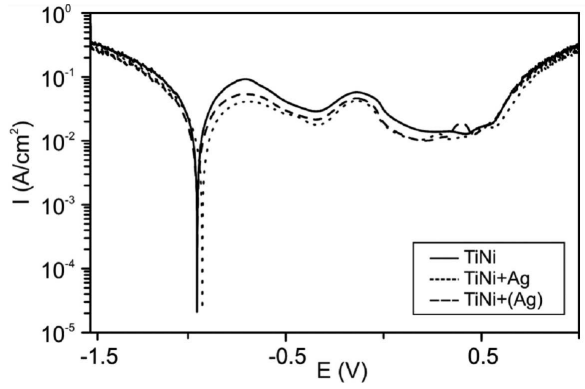

Fig. 4. Potentiodynamic curves of TiNi-based materials in 6 M KOH solution.

Table II and Fig. 5 reports electrochemical properties of studied materials. All electrodes are characterized by good activation properties. The maximum discharge capacity of studied alloys and composite was obtained in 2nd or 3rd cycle. The highest discharge capacity showed TiNi+Ag alloy — 173 mAh/g. MA and annealed TiNi-based materials displayed higher discharge capacity than that the arc ones [9]. Discharge capacities for all studied materials decreased during next cycles of charging and discharging. It is probably caused by formation of

TABLE II

Maximum discharge capacity, capacity retaining rate after 18th cycle, corrosion current of TiNi-based materials.

Composition	Max. discharge capacity [mAh/g]	Capacity retaining rate after 18^{th} cycle [%]	Corrosion current [A/cm^2]
TiNi	171	65	2.33×10^{-2}
TiNi+Ag	173	76	1.79×10^{-2}
TiNi+(Ag)	159	84	1.19×10^{-2}

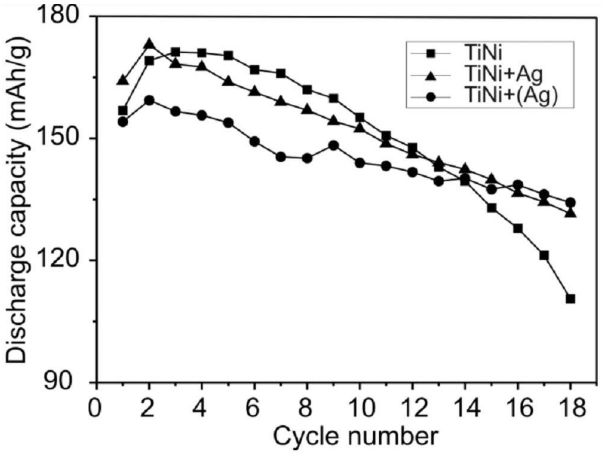

Fig. 5. Discharge capacities as a function of cycle number of electrode prepared with TiNi-based materials (solution 6 M KOH, room temperature).

oxides, hydroxides, and irreversible hydride phases. Created hydroxide layer acted as a barrier for the atomic hydrogen in and out diffusion and the materials electrochemical performance deteriorated with charge/discharge cycles. A positive effect of Ag addition can be related to creation of easy diffusion pathways trough the hydroxide layer for atomic hydrogen. It could be also caused by selective dissolving of hydroxide layer making it more porous and less stable which is favorable for hydrogen transport. TiNi+(Ag) is characterized by the best capacity retaining rate after 18th cycle, which equaled 84%.

4. Conclusions

TiNi-based alloys and composites with Ag prepared by MA and annealing were used as negative electrodes for Ni-MH_x rechargeable batteries. Based on this study the following conclusions can be obtained:

- Chemical modification of TiNi alloy by 5 wt% of Ag element does not affect crystallite size and average agglomerate size.
- Ag particles improves corrosion resistance of TiNi alloy in alkaline solution.
- TiNi with 5 wt% composite is characterized by the best cycle stability during electrochemical tests which equaled 84% after 18 cycles.

References

[1] E. Jankowka, M. Makowiecka, M. Jurczyk, *Renew. Energ.* **33**, 211 (2008).

[2] C.S. Wang, Y.Q. Lei, Q.D. Wang, *J. Power Sources* **70**, 222 (1998).

[3] J. Liu, X.P. Gao, D.Y. Song, Y.S. Zhang, S.H. Ye, *J Alloys Comp.* **231**, 852 (1995).

[4] R.A. Varin, T. Czujko, Z.S. Wronski, *Nanomaterials for Solid State Hydrogen Storage*, Springer, New York 2009.

[5] M. Balcerzak, M. Jurczyk, *Inzynieria materialowa* **5**, 370 (2012) (in Polish).

[6] M. Balcerzak, M. Nowak, J. Jakubowicz, M. Jurczyk, *Renew. Energ.* **62**, 432 (2014).

[7] R.J. Shih, Y.O. Su, T.P. Perng, *J. Alloys Comp.* **353**, 283 (2003).

[8] B. Huang, P. Shi, C. Lu, Z. Liang, M. Chen, *Rare Metal Mater. Eng.* **34**, 557 (2005).

[9] C.B. Jung, K.S. Lee, *J. Alloys Comp.* **253-254**, 605 (1997).